(−)-Epicatechin metabolites promote vascular health through epigenetic reprogramming of endothelial-immune cell signaling and reversing systemic low-grade inflammation

Journal Pre-proofs

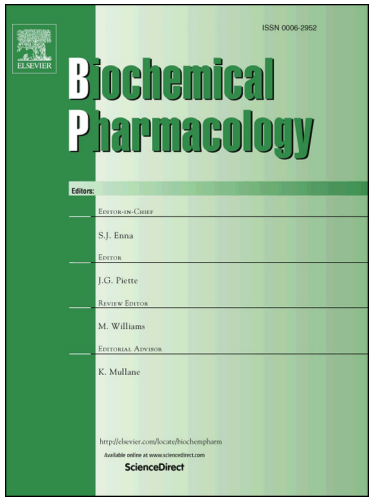

(-)-Epicatechins promote vascular health through epigenetic reprogramming of endothelial-immune cell signaling and reversing systemic low-grade inflammation

Dragan Milenkovic, Ken Declerck, Yelena Guttman, Zohar Kerem, Sylvain Claude, Antje Weseler, Aalt Bast, Hagen Schroeter, Christine Morand, Wim Vanden Berghe

PII: S0006-2952(19)30398-3
DOI: https://doi.org/10.1016/j.bcp.2019.113699
Reference: BCP 113699

To appear in: *Biochemical Pharmacology*

Received Date: 4 July 2019
Accepted Date: 6 November 2019

Please cite this article as: D. Milenkovic, K. Declerck, Y. Guttman, Z. Kerem, S. Claude, A. Weseler, A. Bast, H. Schroeter, C. Morand, W.V. Berghe, (-)-Epicatechins promote vascular health through epigenetic reprogramming of endothelial-immune cell signaling and reversing systemic low-grade inflammation, *Biochemical Pharmacology* (2019), doi: https://doi.org/10.1016/j.bcp.2019.113699

(-)-Epicatechins promote vascular health through epigenetic reprogramming of endothelial-immune cell signaling and reversing systemic low-grade inflammation

Dragan Milenkovic[a,b*#], Ken Declerck[c#], Yelena Guttman[d], Zohar Kerem[d], Sylvain Claude[a], Antje Weseler[e], Aalt Bast[e], Hagen Schroeter[e], Christine Morand[a], Wim Vanden Berghe[c*]

[a] Université Clermont Auvergne, INRA, UNH, CRNH Auvergne, F-63000 Clermont-Ferrand, France

[b] Department of Internal Medicine, Division of Cardiovascular Medicine, School of Medicine, University of California Davis, Davis, California, 95616, United States of America

[c] PPES, Department of Biomedical Sciences, University of Antwerp (UA), Wilrijk, Belgium

[d] Institute of Biochemistry, Food Science and Nutrition, The Robert H. Smith Faculty of Agriculture, Food and Environment, The Hebrew University of Jerusalem, P.O. Box 12, Rehovot 76100, Israel

[e] Department of Pharmacology and Toxicology; Faculty of Health, Medicine and Life Sciences, P.O. Box 616, 6200, MD, Maastricht, The Netherlands

[f] Mars, Inc., McLean, VA

(# equally contributed)

* Corresponding authors:

Dr Dragan Milenkovic, PhD

dragan.milenkovic@inra.fr

Dr Wim Vanden Berghe, PhD

Wim.vandenberghe@uantwerpen.be

Abstract

Ingestion of (-)-epicatechin flavanols reverses endothelial dysfunction by increasing flow mediated dilation and by reducing vascular inflammation and oxidative stress, monocyte-endothelial cell adhesion and transendothelial monocyte migration *in vitro* and *in vivo*. This involves multiple changes in gene expression and epigenetic DNA methylation by poorly understood mechanisms. By *in silico* docking and molecular modeling we demonstrate favorable binding of different glucuronidated, sulfated or methylated (-)-epicatechin metabolites to different DNA methyltransferases (DNMT1/DNMT3A). In favour of this model, genomewide DNA methylation profiling of endothelial cells treated with TNF and different (-)-epicatechin metabolites revealed specific DNA methylation changes in gene networks controlling cell adhesion-extravasation endothelial hyperpermeability as well as gamma-aminobutyric acid, renin-angiotensin and nitric oxide hypertension pathways. Remarkably, blood epigenetic profiles of an 8 week (-)-epicatechin diet intervention in male smokers revealed individual epigenetic gene changes targeting similar pathways as the *in vitro* exposure experiments in endothelial cells. Furthermore, epigenetic changes following (-)-epicatechin diet intervention oppose atherosclerosis associated epigenetic changes. In line with biological data, the individual epigenetic response to an (-)-epicatechin diet is associated with different vascular health parameters (glutathione peroxidase 1 and endothelin-1 expression, acetylcholine response), in part involving systemic shifts in blood immune cell types which reduce the neutrophil-lymphocyte ratio (NLR). Altogether, our study suggests that different (-)-epicatechin metabolites promote vascular health in part via epigenetic reprogramming of endothelial-immune cell signaling and reversing systemic low-grade inflammation.

1. Introduction

Flavonoids are a group of polyphenolic compounds and contribute to the beneficial health effects of fruits and vegetables [1]. In the context of cardiovascular health, flavonoids are of interest, because the habitual intake of flavanols, proanthocyanidins and theaflavins has been associated with reduced coronary artery disease (CAD) risk and mortality [2, 3]. Flavanols consist of monomeric catechin and epicatechin, and oligomeric procyanidins, among others, and have been mainly found in cocoa, apples and tea. Only monomers and dimers are absorbed in the small intestine, and undergo extensive metabolization in the gut and liver leading to glucuronidated, sulphated and methylated epicatechin and γ-valerolactone metabolites [4-6].

Experimental studies and randomized controlled trials (RCTs) further confirm the cardioprotective effects of flavanols [7] including effects on blood pressure [8, 9], vasodilation [9, 10], pulse wave velocity [9] and LDL cholesterol [11]. The most consistent effect is on endothelial function measured by flow-mediated vasodilation (FMD) [12], which is an independent risk factor for cardiovascular diseases. Multiple RCTs showed an increase in FMD and reduction in blood pressure, both in CVD high risk and low risk individuals [9, 13]. This effect is mainly due to the enhancement of NO synthesis and levels in the vascularity [14]. Furthermore, (-)-epicatechin and its circulating metabolite epicatechin-7-O-glucuronide were found the major compounds responsible for this increase in FMD after the consumption of cocoa flavanol-rich diet [7].

Another way how flavanols may beneficial impact endothelial function and prevent cardiovascular diseases is by reducing the recruitment and migration of monocytes into the arterial wall. Accumulated oxidized LDL cholesterol in the intima leads to the expression of varies cell adhesion and chemokine proteins in endothelial cells. Circulating monocytes are subsequently recruited to the endothelial wall and migrate into the intima where they differentiate into macrophages [15]. Previously, we have demonstrated that (-)-epicatechin metabolites decrease pro-inflammatory interactions between monocytes and endothelial cells [16]. Moreover, we demonstrated that monocyte-endothelial cell adhesion and leukocyte rolling induced by an inflammatory stimulus was reduced upon pre-treatment with a mixture of 3 epicatechin metabolites *in vitro* and *in vivo* [17]. Upon integration of transcriptome, miRNAome and DNA methylome profiles of endothelial cells exposed to a mix of (-)epicatechin metabolites, common targeted pathways were identified related to endothelial cell adhesion and transmigration. These results indicate that (-)-epicatechin may prevent monocyte recruitment and transendothelial migration through the modulation of gene

expression, miRNA expression and DNA methylation. Epigenetic effects of (-)-epicatechin metabolites on endothelial DNA methylation provides an attractive working model explaining a potential mechanism of action underlying their health properties because DNA methylation can be seen as an important mediator in memorizing past adverse environmental effects. Indeed, previous studies demonstrated that LDL cholesterol, homocysteine and disturbed blood flow induces DNA methylation changes in endothelial cells [18-20]. It has been suggested that dietary polyphenols promote cardiovascular health by targeting multiple classes of epigenetic writer-reader-eraser enzymes related to histone acetylation-methylation and DNA methylation [21].

The aim of this study was to evaluate whether physiological concentrations of glucuronidated, sulphated or methylated (-)-epicatechin metabolites trigger epigenetic DNA methylation changes related to cardiovascular health *in vitro* and *in vivo* in a diet intervention study.

2. Material and Methods

2.1 (-)-epicatechin flavanol metabolites

(-)-epicatechin metabolites: 4′-*O*-methyl(-)-epicatechin (4'MEC), 4′-*O*-methyl(-)-epicatechin-7-β-D-glucuronide (4'MEC7G) and (-)-epicatechin-4′-sulfate (EC4'S) were gifted by Mars Inc (McLean, VA, USA). Conjugated metabolites were dissolved in 50% ethanol in double distilled water and diluted to a final working concentration of 1 µM in cell medium for cell culture experiments. An 1µM (-) epicatechin mix was prepared containing equimolar fractions of the 3 metabolites. TNFα was obtained from R&D Systems (Lille, France) and was dissolved in 0.1% bovin serum albumin (St. Louis, MA, USA).

2.2 Cell culture conditions

Human umbilical vein endothelial cells (HUVEC) (Lonza, Walkersville, MD, USA) were cultured in a phenol-free endothelial growth medium (EGM) supplemented with 2% fetal bovine serum (FBS), 0.4% fibroblast growth factor, 0.1% vascular endothelial growth factor, 0.1% heparin, 0.1% insulin-like growth factor, 0.1% ascorbic acid, 0.1% epidermal growth factor and 0.04% hydrocortisone (all from Lonza). HUVECs, at passage 4, were seeded into the 24-well plates (BD-Falcon, Le Pont-De-Claix, France) and grown to reach 60-70% confluence. The medium was then replaced to expose the cells for 3h to the culture medium containing either solvent alone (ethanol 0.5‰, control wells, vehicle) or different metabolites: 4′-*O*-methyl(-)-epicatechin, 4′-*O*-methyl(-)-epicatechin-7-β-D-glucuronide or (-)-epicatechin-4′-sulfate at 1µM. At the end of the incubation period, the medium was replaced with flavanol free medium and left for further 18h until confluence. The confluent monolayer was then stimulated for 4 hours with TNFα (R&D Systems Lille, France) at 0.1 ng/mL or only incubated with PBS/BSA (0,001%, negative control). Following gDNA isolation, genomewide DNA methylation profiles were generated by Illumina 450k BeadChip (Illumina, San Diego, CA, USA) arrays covering >450,000 CpG dinucleotides.

2.3 Genomic DNA extraction

Genomic DNA (gDNA) from HUVEC was extracted using DNeasy kit (Qiagen, Courtaboeuf, France). DNA purity and concentrations were determined by UV-VIS spectrophotometry (NanoDrop, Thermo Fisher Scientific Inc, Wilmington, DE, USA) and stored at -80°C until further

use. For each sample 1 µg of gDNA was bisulfite converted using the EZ DNA Methylation kit (Zymo research, Irvine, CA, USA) according to manufacturer's instruction. Successful bisulfite conversion was confirmed by performing a methylation-sensitive PCR in a region of the SALL3 gene. (see [22] for primer sequences).

2.4 DNA-methylation arrays

Bisulfite converted DNA from the HUVECs was hybridized to the Illumina HumanMethylation450 BeadChip arrays (Illumina, San Diego, CA, USA). Briefly, for each sample, 1 µg of genomic DNA was bisulfite-converted using an EZ DNA methylation Kit (ZYMO research, Irvine, CA, USA) according to the manufacturer's recommendations. Converted gDNA was eluted in 22 µl of elution buffer. DNA methylation level was measured using the Illumina Infinium HD Methylation Assay (Illumina, San Diego, CA, USA) according to the manufacturer's instructions. Briefly, 4 µl of bisulfite-converted DNA (±150 ng) was isothermally amplified overnight (20–24h) and fragmented enzymatically. Precipitated DNA was resuspended in hybridization buffer and dispensed onto the Infinium HumanMethylation450 BeadChips (12 samples/chip) using a Freedom EVO robot (Tecan, Männedorf, Switzerland). The hybridization procedure was performed at 48°C overnight (16–20 h) using an Illumina Hybridization oven. After hybridization, free DNA was washed away and the BeadChips were processed through a single nucleotide extension followed by fluorescent readout of the incorporated base using a Freedom EVO robot. Finally, the BeadChips were imaged using an Illumina iScan (Illumina, San Diego, CA, USA). Raw Illumina450K data have been deposited in the GEO-profile database as GSE133418 (in vitro methylation data), GSE107143 (atherosclerosis methylation data) [23] and GSE54643 (epicatechin diet intervention methylation data) [24]. Detection p-values were calculated to identify failed probes as per Illumina's recommendations. No arrays exceeded our quality threshold of >5% failed probes. Filtering of bad quality probes and normalization of raw methylation beta values was conducted using RnBeads package in R software [25]. Probes with detection p-values higher than 0.01, overlapping with SNPs at the last 3 bases in its sequence or containing missing values were excluded. Beta mixture quantile dilation (BMIQ) was used to normalize between the two different probe designs (Infinium I and Infinium II) [26]. Differentially methylated probes were identified using moderated t-test in the limma R package. Probes with a p-value below 0.01 and a methylation difference of at least 5% were defined as differentially methylated probes (DMPs). Probes were assigned to genes, CpG

island annotations (CpG island, CGI shores, CGI shelves, and open sea) and gene regions (TSS1500, TSS200, 5'UTR, 1st exon, gene body and 3'UTR) based on the HumanMethylation450 v1.2 Manifest file from Illumina. Probes were also mapped to chromatin segmentation states obtained from the UCSC genome browser. Enrichment of DMPs in different genomic regions was measured by the Fisher's Exact test. Blood cell type composition was estimated using the reference-based method of Houseman with the EpiDISH R package [27, 28]. All analyses were performed in R and R Studio. Epigenetic age was estimated using the epigenetic clock of Horvath [29].

2.5 Bioinformatic analysis

DMPs were mapped to genes according the HumanMethylation450 v1.2 Manifest file from Illumina. Corresponding gene lists were used to perform pathway enrichment analysis using Ingenuity Pathway Analysis (IPA) software, KEGG (Kyoto Encyclopedia of Genes and Genomes) (http://www.genome.jp/kegg/tool/map_pathway2.html) and Metacore software packages Metacore™ (GeneGo, St Joseph, MO, USA; https://portal.genego.com). Enrichment statistics were calculated for these data sets assuming a hypergeometric distribution to identify significantly overrepresented pathways. Canonical pathways were considered significant overrepresented when they had a Fisher's Exact p-value < 0.05. Venn diagrams were created using the VennDiagram R package. Partial Least Squares Discriminant Analysis (PLS-DA) multivariate analysis was performed using the mixOmics R package. Gene network analyses were searched using text-mining algorithm of MetaCore software from Clarivate Analytics (https://portal.genego.com). To identify pathways that are significantly associated with the genes, we used the web tool GeneTrail2 (https://genetrail2.bioinf.uni-sb.de/) [30], version 1.6, as a platform to access KEGG and BioCarta databases. Interactions between functional groups of genes were searched using the online tool Metascape (http://metascape.org) [31]. The obtained network was further visualized using Cytoscape platform for molecular interaction networks visualization (https://cytoscape.org/) [32]

2.6 mm-GBSA binding affinity calculations

2.6.1 Preparation of proteins and ligands: The atomic coordinates of both human DNMT1 and DNMT3A proteins were retrieved from the Protein Data Bank (PDB, https://www.rcsb.org). Chain A of 4WXX crystal structure was chosen for the docking simulations of DNMT1. In the absence

of a full protein crystal structure of DNMT3A, 3LLR and 4U7T crystal structures were chosen to study amino acids 275-427 and 476-912, respectively. Proteins were prepared for docking using the default parameters of Protein Preparation Wizard implemented in Maestro, 2017-4 version (Schrödinger, New York, NY, USA). Ligand 2D structure was retrieved from PubChem database (https://pubchem.ncbi.nlm.nih.gov, NIH, Bethesda, MD, USA) as SDF. (-)-epicatechin, 4'MEC, 4'MEC7G and EC4'S, sucrose and naphthalene have a PubChem CID of 72276, 11420256, 131750802 71579043, 5988 and 931, respectively. Ligands' 3D structure was generated using the LigPrep command in Maestro.

2.6.2 Docking model and mm-GBSA calculation: The sitemap algorithm (Schrödinger, New York, NY, USA) was used to determine five possible docking sites of DNMT1, which were later identified by comparing to domain information from UniProt (https://www.uniprot.org). 3PTA a crystal structure of DNMT1 in complex with DNA was used as a reference to the DNA binding domain of the DNMT1. Three of the predicted binding sites, a site at the DNA binding domain and two sites at the catalytic domain were chosen for further analysis. Four binding sites were determined For DNMT3A. 3LLR is the crystal structure of the histone binding PWWP domain. A grid of the histone binding site was generated based on the centroid of histone H3 peptide from the 5CIU crystal structure of DNMT3B PWWP domain in complex with H3. In addition, three binding sites of DNMT3A were determined by the protein interactions in the 4U7T crystal structure of the heterotetramer DNMT3L-DNMT3A-DNMT3A-DNMT3L in complex with histone H3. A grid of the histone binding site was generated based on the centroid of histone H3 peptide. Grids of DNMT3A-DNMT3L and DNMT3A-DNMT3A binding sites were generated as a centroid of DNMT3L (chain b) and DNMT3A (chain c) amino acids in a range of 3Å from DNMT3A (chain a), respectively. In each site, default Glide options for extra precision were used for the docking model with the exception of using 30 poses for the number of poses to include and ten poses for the number of poses to write out. For each ligand, docking pose with the lowest Glide emodel score was selected for further analysis. Binding free energy was calculated using the Prime mm-GBSA package (Schrödinger, New York, NY) as follows: $\Delta G(bind) = E(complex) - [E(ligand) + E(receptor)]$

3 Results

3.1 In silico modeling of different (-)-epicatechin metabolites to DNMT1 and DNMT3A reveals favorable binding modes.

Based on *in silico* models of (-)epicatechin binding to DNMTs in nutriepigenetic studies with green tea [33, 34], we compared DNMT binding properties of different (-)-epicatechin metabolites identified in cocoa flavanol diet intervention studies, i.e. 4′-*O*-methyl(-)-epicatechin (4'MEC), 4′-*O*-methyl(-)-epicatechin-7-β-D-glucuronide (4'MEC7G) and (-)-epicatechin-4′-sulfate (EC4'S) (**Figure 1A**). Using the sitemap algorithm, we were able to predict five potential docking sites in DNMT1 (**Figure 1B-G**), of which only those located at regions with defined function were selected for the docking simulation: one site located at the DNA binding site of the protein and two sites located at the catalytic domain. DNMT3A is active as a hetero-tetrameric (DNMT3L-DNMT3A-DNMT3A-DNMT3L) protein. Four docking sites were determined from the 3D structure: the PWWP domain, usually found in DNA-binding proteins, the H3 histone binding site and two protein-protein interaction sites (DNMT3A-DNMT3A and DNMT3A-DNMT3L) (**Figure 1E-H**). Using docking simulation, we propose possible binding modes of of EC4'S in both active sites and regulatory regions of DNMT1 and DNMT3A (shown in enlarged rectangle). Hydrogen bonds are represented as light blue dashed lines **(Figure 1B-H**).

The mm-GBSA method serves for ranking ligands with similar scaffold according to their calculated binding affinity [35]. One way to validate the calculation-based predictions is to demonstrate their specificity to the active molecules in question. We have calculated the binding potential of sucrose, an H-bond donor-rich molecule, and of naphthalene, a hydrophobic molecule, both without effect on the mechanisms discussed here, as a benchmark for metabolites' binding potency. Our predictions demonstrate the highest binding affinities to most of the tested binding sites for one metabolite, i.e., 4'MEC7G (**Table 1**). The calculated binding energy (ΔG) of 4'MEC7G was 12.83-34.76 kcal/mol lower than of the control molecules, in all sites except for one site located in the DNMT1 catalytic domain. However, both 4'MEC and MEC4'S presented potential affinities for DNA binding site but not for catalytic domain I and II. Interestingly, epicatechin metabolites present higher affinities for DNMT1 than the parent compound. As for DNMT1, 4MEC7G was also predicted to have highest affinity for DNMT3A, with calculated binding energy (ΔG) of 4MEC7G estimated to be 13.27-29.61 kcal/mol lower than of the control

molecules for all 4 tested sites. In our analyses, 4'MEC presented the highest binding affinity for PWWP domain and EC4'S H3 peptide binding site (**Table 1**).

3.2 (-)-Epicatechin metabolites trigger common endothelial DNA methylation changes opposite to TNF treatment

Previously, (-)-epicatechin specific inhibition of DNMT activity has been demonstrated *in vitro* for Ss1 DNMT and human DNMT1 enzymes, with IC50 values of respectively 8.1 and 8.4 μM [34]. Here, we further compared epigenetic DNA methylation changes in TNF treated HUVEC cells, either or not, following pretreatment with each of the 3 different (-)-epicatechin metabolites. Briefly, subconfluent HUVEC cells were exposed for 3 h to control medium (i.e. culture medium with 0.5‰, ethanol solvent) or culture medium containing 1μM of individual flavanol metabolites 4′-*O*-methyl(-)-epicatechin (4'MEC), 4′-*O*-methyl(-)-epicatechin-7-β-D-glucuronide (4'MEC7G) or (-)-epicatechin-4′-sulfate (EC4'S), which corresponds with maximum plasma concentrations of metabolites detected in cocoa diet intervention studies [17, 36-38]. After 3h (-)-epicatechin treatment, the medium was replaced with flavanol free medium and left for 18h untreated, before adding TNFα for 4h. Following gDNA isolation and bisulfite treatment, genomewide DNA methylation profiles were generated by Illumina 450k BeadChip arrays covering >450,000 CpG dinucleotides (GSE133418) [17]. Reliability of our DNA methylation profiling approach was confirmed upon comparing the endothelial DNA methylation profile of HUVEC control cells with independent HUVEC DNA methylation profiles available in the ENCODE dataset GSE82234, which revealed highly significant correlation (Pearson correlation > 0.98) [17] (data not shown). Next, partial least squares discriminant multivariate analysis (PLS-DA) of epigenetic profiles revealed clear separation between untreated cells (control), TNF treated cells, and TNF treated cells following (-)-epicatechin metabolite pretreatment (**Figure 2A**). More specifically, 4h TNFα treatment elicits significant DNA methylation. changes ($P < 0.01$ and Δ β-value > 0.05) of 559 hypermethylated and 198 hypomethylated CpG probes (**Figure 2B**). Since the profiles of the 3 (-)-epicatechin metabolites 4'MEC, 4'MEC7G and EC4'S clustered together, this suggests clear similarities in DNA methylation changes by the different epicatechin metabolites.

Pretreatment of endothelial cells to 4'MEC, 4'MEC7G or EC4'S followed by TNF treatment (**Figure 3B**) triggered respectively hypomethylation of 393, 740 and 548 CpG and hypermethylation of 313, 902 and 848 CpG probes as compared to TNF treatment alone (**Figure**

2B). Analyses of the methylation changes across chromosomes in a Manhattan plot showed a widespread distribution across the genome (**Figure 2C**). More particularly, we observed an enrichment of differentially methylated probes (DMPs) in intergenic regions, and a depletion in regions around the transcription start site (TSS) of genes when compared to all the Illumina CpG probes (**Figure3A**). Along the same line, mapping DMPs to chromatin states confirmed a depletion in promoter states. Especially hypo-DMPs were slightly enriched in gene bodies and 3'UTRs. Both hypo- and hyper-DMPs were found to be depleted in CpG islands, and were therefore mainly located in CpG-poor regions. DMPs were weakly enriched in enhancer regions, although significance ($p<0.05$) could not be reached in all contrasts. An enrichment of DMPs in heterochromatin states was found for all contrasts.

To check whether the hyper- or hypomethylation changes were similar between the 3 different flavanol metabolites and TNF versus TNF treatment alone, the -log10(p-values) of each probe were calculated for each contrast and made negative when hypomethylated and kept positive when hypermethylated. Upon comparing these -log10(p-values), strong positive Pearson correlations were found across the different metabolites (r between 0.47 and 0.51) (**Figure 3B**), indicating that the 3 different flavanol metabolites induce similar epicatechin specific DNA hyper/hypomethylation changes in line with the PLS-DA analysis (**Figure 2A**). In contrast, when comparing epigenetic changes of each (-)-epicatechin metabolite and TNF versus TNF treatment with epigenetic changes of TNF treatment versus control cells, a negative Pearson correlation (r between -0.26 and -0.33) was found between the -log10(p-values). This indicates that in general the 3 (-)-epicatechin metabolites trigger opposite epigenetic changes in comparison to TNF induced DNA methylation effects (**Figure 3C**).

3.3. (-)-Epicatechin metabolites trigger common endothelial DNA methylation changes in genes involved in cell adhesion, cytoskeletal organization, renin angiotensin, nitric oxide hypertension and axonal guidance signaling pathways

We further applied respectively Metacore gene network, KEGG and Ingenuity pathway enrichment analysis on DMP associated gene lists of the 3 different (-)-epicatechin metabolite treatments and TNF combination treatments relative to TNF treatment alone, which identified 81 common differentially methylated target genes (Figure 4A). The enriched gene networks (**Figure 4B**) and pathways (**Figure 4C-D**) were ranked again based on the sum of the -log10 enrichment

p-values, in each treatment contrast. In this way, networks or pathways which are enriched in more than one contrast are therefore in common across the treatments and ranked first. Among the top ranked pathways, we found interesting pathways including cell adhesion, axonal guidance, netrin, ephrin and integrin signaling, actin cytoskeletal signaling, vascular morphogeness, hedgehog and wnt signaling. These enriched pathways are involved in various aspects of atherogenesis via eliciting endothelial dysfunction, monocyte attraction, leukocyte infiltration, monocyte-macrophage retention, platelet hyperreactivity, and neovascularization [39-43]. Moreover, the results are in line with previously obtained *in vitro* and *in vivo* biological data, showing that epicatechin metabolites mediate their vasculoprotective effects through dynamic regulation of endothelial cell monocyte adhesion and permeability [17]. IPA pathway analysis (**Figure 4D**) also identified significant gamma-aminobutyric acid (GABA) and pathway enrichment in response to the 3 (-)-epicatechin metabolites. Recent evidence revealed a neuro-cardioprotective role for GABA against oxidative endothelial injury and regulation of endothelial nitric oxide eNOS [44, 45]. Also renin-angiotensin and nitric oxide signaling pathways are enriched which play critical roles in hypertension and may contribute in cardioprotective blood pressure-lowering effects of (-)-epicatechins [12, 46-48]**.** Endocrine flavanol functions are suggested via regulation of gonadotropin receptor hormone (GnRH) and androgen receptor (AR) signaling, involved in plaque stabilization and/or rupture [49-51]. Finally, integrated Metascape protein network analysis revealed various links between the different (-)-epicatechin specific biological processes related to focal adhesion, signal transduction, cancer development, G-alpha protein signaling and axon guidance (**Figure 4E**).

3.4. (-)-Epicatechin metabolites and TNF trigger opposite endothelial DNA methylation changes in cell junction associated genes

Out of 81 epicatechin specific gene associated DMPs (**Figure 4A**), we identified 26 genes for which opposite methylation changes were detected by at least one (-)-epicatechin metabolite in comparison to TNF treatment alone (USP35, PCDHGA1, SMOC2, SDK1, SKI, GLUD1P3, SOX1, DOCK5, AKAP12, PTPRN2, NLGN1, FLJ38576, TNXB, DLGAP2, SLC38A4, BANP, LAS1L, XKR4, DACT1, SYNPR, FTCDNL1, GLI3, PCDH9, PTCHD3, ERICH1-AS1, KDM2B) (**Figure 5A**). Besides, TNF induces also multiple DNA methylation changes which are not responsive to (-)-epicatechin treatment (**Figure 5A**). Heatmap analysis of DNA methylation changes of these 26

genes identified 2 major clusters of opposite DNA methylation changes by TNF and the 3 (-)epicatechin metabolites (**Figure 5B**). Cluster 1 reveals 5 hypomethylated TNF responsive genes, which remain hypermethylated upon pretreatment with the 3 (-) epicatechin metabolites (**Table 2**). The opposite pattern can be seen in cluster 2, showing 11 hypermethylated TNF responsive genes, which remain hypomethylated upon pretreatment with the 3 (-)-epicatechin metabolites, as illustrated for the gene USP35 (**Table 3**) (**Figure 5C**). Pathway enrichment analysis of the shortlist of 26 genes, reveals significant enrichment of cell junction regulation (GO:0030054, P-value=9.470×10^{-3}), which is critically involved in endothelial permeability and transendothelial monocyte migration [16, 17]. Endothelial cell–cell junctions are critical for vascular integrity, whereas their dysfunction and endothelial hyperpermeability represents an initiating step in early atherosclerosis and coronary artery disease [52-54]. In support of our results, TNF has previously been shown to increase endothelial permeability and promote monocyte transendothelial migration, whereas (-)-epicatechin (pre)treatment antagonizes inflammation associated endothelial hyperpermeability [17, 55-57].

3.5. Individual DNA methylation response of (-)-epicatechin diet intervention targets genes involved in cell adhesion, cytoskeletal organization, renin angiotensin, nitric oxide hypertension and axonal guidance signaling pathways

A double-blind, randomized, placebo-controlled intervention study revealed that the daily consumption of monomeric and oligomeric (-)-epicatechin flavanols (MOF) derived from seeds of grapes (*Vitis vinifera* L.) for 8 weeks accomplishes a vascular health benefit in male smokers [58]. Corresponding DNA methylation levels of blood samples were measured before and after the diet intervention using the 450k Illumina array platform, but no common diet responsive CpG probe was found to be differentially methylated due to strong interindividual epigenetic variation in baseline methylation levels and variable response to a (-)-epicatechin rich diet intervention [24] (GEO-data available at GSE54690). Upon reanalysis, we now selected probes that changed in methylation by at least 0.1 in beta-value (corresponding with >10% methylation change) after epicatechin diet intervention for every individual participant of the study. We noticed that some individuals (SN_110, SN_109 and SN_114) showed a strong epigenetic response with a total number of DMPs between 5,469 and 15,189, while other individuals showed much less difference in methylation changes after the (-)-epicatechin intervention (**Figure 6A**). We could not

identify a common CpG probe which was differentially methylated in every individual and only a small fraction of the probes was affected in more than one individual (**Figure 6B**). Next, we performed IPA pathway analysis for every individual for the corresponding CpG probes that showed a change in methylation of at least 10%. To compare the enriched pathways among the individuals, we ranked the pathways based on the sum of the -log10 enrichment pvalues in each individual. In this way, the pathways which were enriched in more than one individual were ranked first (**Figure 6C**). In addition, -log10 enrichment pvalues of pathway analysis of the *in vitro* experiments with the different (-)-epicatechin metabolites or a mix thereof were included and cluster analysis was formed (**Figure 6C**) Remarkably, among the top ranked pathways, we could find several common enriched pathways of interest, including leukocyte extravasation signaling, axonal guidance signaling, netrin signaling, thrombin signaling, GABA, GnRH and nitric oxide signaling, similar to the *in vitro* treatment experiments. Despite the significant enrichment ($p < 0.05$) of various pathways across different individuals, no common differentially methylated genes could be identified in response to the diet intervention (data not shown) [24]. This suggests highly redundant gene networks to control cell adhesion and leukocyte extravasation.

3.6. Individual DNA methylation response of (-)-epicatechin diet intervention associates with cardioprotective vascular health biomarkers.

Since the cardioprotective role of (-)-epicatechin flavanols is well established (see introduction), we first evaluated whether atherosclerosis and flavanol diet intervention associated DNA methylation profiles show opposite methylation direction. We therefore compared the mean DNA methylation differences after the diet intervention with the DNA methylation signature of atherosclerotic patients (athDMPs) [23]. Interestingly, based on the mean delta betas (indicates degree of DNA Methylation difference) of all individuals, a negative correlation ($r=-0.41$) was found with the delta betas of the athDMPs , suggesting that (-)-epicatechin treatment elicits opposite DNA methylation changes than atherosclerosis progression (**Figure 7A**). Hypomethylated athDMPs were on average increased in methylation after the (-)-epicatechin diet intervention, wheres hypermethylated athDMPs were mainly decreased in methylation. Furthermore, when calculating the correlation between delta betas in every individual separately, we found more individuals with negative correlation (i.e. cardioprotection) than with positive correlations (i.e. proatherogenic) (**Figure 7B**). Especially individuals SN_114, SN_109 and

SN_110 demonstrated a strong negative cardioprotective correlation. Interestingly, the three samples (SN_114, SN_109 and SN_110) with the strongest DNA methylation response (highest number of DMPs) (SN_114, SN_109 and SN_110) were also the most negatively correlated with the athDMPs.

Since blood is a heterogeneous collection of different cell types, each characterized by unique DNA methylation profile, we next applied the houseman algorithm to estimate blood cell type composition before and after diet intervention in every individual [27]. This algorithm allows mathematical deconvolution of relative immune cell type composition of blood samples based on Illumina 450k data [59]. In line with this prediction model, increased fraction of neutrophil granulocytes and reduced fraction of CD4+T lymphocyte cells have already been reported in atherosclerosis patients in comparison to control individuals [23]. Interestingly, the (-)-epicatechin diet intervention promotes predominantly opposite shifts in cell type composition, based on the Pearson correlation coefficients of (-)-epicatechin DMPs of the different individuals versus atherosclerosis athDMPs (**Figure 7C**). For example, DMPs of individual SN_114 with the strongest negative athDMP correlation coëfficient showed the biggest reduction in granulocyte fraction but highest increase of CD4+T cell fraction. This houseman prediction could be further experimentally confirmed with the vascular health biomarkers which have been monitored in these individuals [58] (**Figure 8A**). When comparing the individual pearson correlation coefficient of epicatechin DMPs versus athDMPs, the strongest positive correlation was found for the neutrophil counts and the most negative correlation was found for the lymphocyte counts. In case of a negative pearson correlation efficient of epicatechin diet DMPs versus athdMPs , this corresponds with reduced neutrophil counts and increased lymphocyte counts, in line with the houseman algorithm prediction. This suggests that epigenetic reprogramming of adaptive immunity of neutrophil and T cell populations in response to (-)-epicatechin might also significantly contribute to its cardioprotective properties.

We next checked to what extent epigenetic responders of the (-)-epicatechin diet could be correlated with additional vascular health parameters. For this, correlations were performed between the total number of DMPs and all the micro and macro vascular biomarkers which have been monitored in these individuals [58] (**Figure 8B**). The most significant positive correlations were found for GPX1 expression values and acetylcholine response which increased with higher number of DMPs following (-)-epicatechin diet intervention. Epicatechin is known to improve the

impaired endothelium-dependent relaxation response to acetylcholine [60]. GPX1 is involved in oxidative stress defense mechanisms [61]. GPX1 deficiences play a critical role in cardiac dysfunctions and AngII-dependent hypertension, but GPX1 activity can be restored upon epicatechin treatment [62, 63]. Besides, GPX1 also regulates epigenetic DNA hydroxymethylation following oxidative stress [64]. The most negative correlations were found for endothelin-1 (ET1) levels which decreased with increasing number of (-)-epicatechin responsive DMPs. ET1 is playing a critical role in cardiovascular hypertension. Of special note, epicatechin is known to lower ET-1 release [60]. How changes in GPX1 an ET1 expression modulate DNA (hydroxy)methylation changes (or vice versa) needs further investigation. Finally, no significant association could be found between the (-)-epicatechin specific DNA methylation response and the total vascular health index, which is an integrative measure of vascular health combining the results from all the vascular biomarkers measured (**Figure 8A-B**) [58]. This suggests that not all measured vascular health parameters are under epigenetic DNA methylation control.

4. Discussion

(-)-Epicatechins are protective against cardiovascular diseases and improve vascular health, however, the underlying mechanism is not fully elucidated. Using molecular modeling and in silico docking, energetically favorable binding was demonstrated of 3 different (-)-epicatechin metabolites with potential docking sites in DNMT1 and DNMT3A/B enzymes. Moreover, in endothelial HUVEC cells, the 3 (-)—epicatechin metabolites induced similar DNA methylation changes, across the different flavanol metabolites. Surprisingly, the CpG sites that changed after (-)-epicatechin treatment were rather enriched in intergenic regions and gene bodies, as compared to promoter regions. Since few promoters changed their methylation status following (-)-epicatechin treatment, only a limited number of genes were found to be both differentially expressed and methylated [17]. Although additional chromatin dependent promoter regulation cannot be excluded [65], (-)-epicatechin specific DNA methylation changes may alternatively modulate long-term transcriptional responses upon repetitive exposure to accumulate a particular DNA methylation threshold [66]. Besides, it also needs to be further investigated whether (-)-epicatechin specific DNA methylation may have additional roles in alternative RNA splicing or regulation of ncRNAs [67-70]. We found that the intergenic and gene body localized DMPs are enriched for genes involved in cell adhesion related pathways, including axonal guidance signaling, paxillin

signaling, netrin signaling, integrin signaling, and actin cytoskeleton signaling. Of particular interest, the role of alternative RNA splicing and noncoding microRNAs in regulation of cell adhesion-motility is increasingly recognized [17, 71-73]. These results are in accordance with previous functional studies showing reduced monocyte-endothelial cell-cell adhesion after epicatechin treatment *in vitro* and *in vivo* [17]. The recruitment and migration of monocytes into the arterial wall is one of the key initial processes during the development of an atherosclerotic plaque. Furthermore, our data also identified (-)-epicatechin specific epigenetic regulation of GABA, renin-angiotensin and nitric oxide pathways controlling blood pressure, as well as endocrine responses via GnRH and AR, which may prevent plaque ruptures [44, 45]. Furthermore, we found that the 3 (-)-epicatechin metabolites can counteract TNF induced epigenetic regulation of 2 gene clusters involved in cell junction regulation, controlling endothelial permeability. This is a critical determinant of leukocyte extravasation and transendothelial migration and can be inhibited by (-)-epicatechins [17, 52-57]. Altogether, we identified TNF-dependent as well as TNF-independent epigenetic changes in multiple pathways associated with cardioprotective properties.

When further trying to identify an (-)-epicatechin specific DNA methylation signature *in vivo* in blood samples of male smokers following an eight-week (-)-epicatechin diet intervention, we presumably failed because of strong interindividual epigenetic variation in lifestyle factors (nutrition, stress, exercise, smoking behavior, age), the limited duration of the diet intervention (8 weeks intervention is short relative to atherosclerosis development over years) and the relative small sample sizes analyzed, (too limited statistical power) [24]. However, upon reanalyzing (-)-epicatechin specific DNA methylation responses at the individual level, we observed significant gene enrichment of common pathways related to cell adhesion and leukocyte extravasation, GnRH, GABA, renin-angiotensin and nitric oxide signaling across all individuals, similar to the *in vitro* results of (-)-epicatechin exposure in the endothelial cell model. Of particular interest, heatmap clustering of these pathway enrichment results of individual epigenetic responses to (-)-epicatechin *in vitro* and *in vivo* reveals that some individual profiles are more similar to 4'MEC and EC4'S metabolite treatment, whereas other individuals are more similar to treatment with 4'MEC7G (-)-metabolite or an equimolar mixture (1μM) of the 3 metabolites. Indeed, interindividual variation in (-)-epicatechin metabolization in the gut-microbiome [6, 9, 74] and/or metabolite specific pharmacodynamics [75] may further expand variation of epigenetic gene responses to (-)-

epicatechin diet intervention [33, 34]. Remarkably, the common pathways identified seem to be robust and tolerate strong interinvidivual epigenetic variation through redundant gene networks.

Upon analyzing vascular health benefits of (-)-epicatechin specific epigenetic changes, Pearson correlation studies showed that individual DMP profile of an (-)-epicatechin diet intervention oppose adverse epigenetic marks associated with atherosclerosis (ath-DMP signature). Moreover, the houseman deconvolution algotrithm revealed that part of the observed DNA methylation changes correspond with decreased neutrophil granulocyte and increased CD4+T-lymphocyte cell counts. The neutrophil-lymphocyte ratio (NLR) is a measure of systemic inflammation and is a known prognostic and predictive marker for cardiovascular diseases. A higher NLR has been associated with increased cardiovascular risk and hypertension [76-79]. As such DNA methylation based estimation of small shifts in immune cell counts and activation status could become an attractive immunomethylomic measure for chronic systemic inflammation, cardiovascular risk and hypertension, similar to NLR based cancer prediction markers [78, 80]. Along the same line, C-reactive protein (CRP), another systemic inflammation marker, was found associated with blood DNA methylation changes of 218 CpGs, of which at least 51 CpGs are related to cardiometabolic health [81]. From a cardioprotective perspective, a polyphenol rich (Mediterranean) diet was reported to lower NLR and chronic inflammatory markers, including CRP [82-88]. Similarly, our DNA methylation results indicate that an (-)-epicatechin diet intervention lowers NLR in various individuals, in favour of cardioprotection. These results could also experimentally be confirmed by vascular health measurements, showing decreased neutrophil granulocyte and increased T-lymphocyte counts following (-)-epicatechin diet intervention. It can therefore be concluded that changes in systemic low grade inflammation or its reduction by (-)-epicatechin can be detected in blood DNA methylation profiles and NLR-specific methylation DMPs may become an attractive blood surrogate biomarker for cardiovascular health.

Besides, we also found significant Pearson correlations for total number of epicatechin responsive DMPs with Gpx1 and ET1 expression levels and acetylcholine response. Experimental data suggest that antioxidative GPx-1 activity modulates cardiovascular risk associated with homocysteine plasma levels, which is linked to methyldonor metabolism supplying S-adenylmethionine donors for DNA methylation [89]. Similarly, homocysteine exerts deleterious effects on endothelial function and vascular tone via release of ET1 [90, 91]. In this respect, epicatechins may promote indirect DNA methylation effects by increasing homocysteine

catabolism (reduced hyperhomocysteinemia) and reshaping the methyldonor metabolism [92]. Assocations with other vascular health markers of interest (such as fmd, aggregation, VCAM, CRP) did not reach significance ($P>0.05$), presumably due to the small sample cohort size and underpowered statistics and may become significant in larger cohort studies.

Because all study participants were heavy smokers, we also tested whether the epicatechin diet could reverse adverse smoking-induced DNA methylation [93]. However, no clear reversal of the smoking methylation pattern could be observed when comparing average methylation changes of the diet intervention and smoking related methylation changes (data not shown). Finally, we also checked whether the (-)-epicatechin diet could rejuvenate the epigenetic age measured by the epigenetic clock of Horvath [29]. However, besides some weak individual rejuvenation effects, no statistical significant change in epigenetic age could be observed at the population level after 8 week diet intervention (data not shown). Similarly, in a recent study, benefits of dietary intervention are limited when started in old age, owing to the development of an inflexible nutritional memory [94].

In conclusion, our results provide solid biochemical evidence that (-)-epicatechins elicit DNA methylation changes in endothelial cells *in vitro* and in a diet intervention study *in vivo*. Characterisation of the corresponding DMPs revealed targeting of common cell adhesion-extravasation signaling pathways, axonal guidance, GABA, renin-angiotensin and nitric oxide hypertension pathways, associated with various cardiovascular health parameters (Gpx1, ET1, acetylcholine response and a decreased neutrophil/lymphocyte ratio). Prolonged longitudinal diet intervention studies in larger study cohorts may allow to evaluate longterm persistence of epicatechin specific epigenetic changes in relation to its cardioprotective properties.

Acknowledgements

We thank the Mars Inc. for providing us with metabolites.

Figure legends

Figure 1: In silico docking analyses of epicatechin metabolites to DNMT1 and DNMT3A. A) Chemical structures of 4'MEC, EC4'S and 4'MEC7G metabolites B) DNA binding site of DNMT1. C,D) catalytic domains of DNMT1. E) PWWP domain of DNMT3A. F) H3 peptide binding site of DNMT3A. G) DNMT3A dimerization site. H) DNMT3L-DNMT3A binding site. The pose of EC4'S in each binding site is shown in enlarged rectangle. Hydrogen bonds are represented as light blue dashed lines.

Figure 2: DNA methylation changes (DMPs) of HUVEC cells upon exposure to epicatechin metabolites and TNF relative to TNF treatment alone. A) Multivariate PLS-DA plot of the first two components showing clear separation of the different treatment conditions. B) Volcano plots revealing CpG probes with significant changes in DNA methylation status. The x-axis shows the mean DNA methylation difference (Δ β-value), whereas the y-axis shows the –log10 of the P-value for each probe, representing the strength of association. Green and red dots represent the hypo- and hypermethylated probes, respectively. The numbers of hyper- and hypomethylated sites are indicated in the plot. C) Manhattan plots showing the differentially methylated sites in each treatment contrast. Red means hypermethylated, green means hypomethylated.

Figure 3: Comparison of DMPs in response to different epicatechin metabolites and TNF relative to TNF treatment alone A) Genomic enrichment of differentially methylated sites. In the heatmap, the log2 enrichment ratio is given comparing the sig-DMPs with all the probes on the Illumina array for different genomic regions (left: gene elements, middle: CpG island elements, right: chromatin state segmentations). Enrichment of the genomic regions was calculated using the Fisher's Exact test: * $p<0.05$, ** $p<0.01$, *** $p<0.001$, **** $p<0.0001$. B) Scatterplots comparing the -log10 (pvalues) of each DMP across the different epicatechin metabolites (4'MEC, 4'MEC7G and EC4'S) and TNF relative to TNF treatment alone. Spearman's correlation coefficients are given. C) Scatterplots of the -log10 (pvalues) of each DMP comparing epicatechin metabolite effect (4'MEC, 4'MEC7G and EC4'S) and TNF against TNF treatment alone versus DMPs of TNF treatment against untreated control. Spearman's correlation coefficients are given.

588 **Figure 4: Pathway enrichment analysis of common gene associated DMPs in response to 3**
589 **different epicatechin metabolites and TNF versus TNF treatment alone.** A) Venn diagram of
590 the overlapping gene associated DMPs across the 3 (-)-epicatechin metabolite contrasts. B)
591 Metacore enriched gene networks C) KEGG enriched pathways C) Metascape protein network
592 analysis network. Circles present different pathways, color represent metabolites that affected
593 methylation level, red for 4'MEC, blue for 4'MEC7G, green for EC4'S. D) Ingenuity pathway
594 enrichment analysis. Top 40 most significantly enriched IPA canonical pathways across the 3 (-)-
595 epicatechin metabolites. The heatmap represents the -log10(p-value) of the enriched pathways.
596 Pathways were ranked by the sum of -log10(p-values).
597
598 **Figure 5: Epicatechin metabolites counteract TNF induced DNA methylation changes.** A)
599 Venn diagram showing the overlapping differentially methylated genes across the different
600 treatment contrasts. B) Heatmap showing the methylation differences of the 26 common genes,
601 including 2 gene clusters. Green means hypomethylation, while red means hypermethylation. C)
602 Example plot of DMP in USP35.
603
604 **Figure 6: Blood DMPs and corresponding pathway enrichment analysis of common gene**
605 **associated DMPs after an 8-week (-)-epicatechin diet intervention in male smokers. A)**
606 Number of DMPs (delta beta-value| > 0.1, i.e. DNA methylation change > 10%). **B)** Number of
607 probes differentially methylated in one or multiple individuals. **C)** Ingenuity pathway enrichment
608 analysis. Top 40 most significantly enriched IPA canonical pathways across the 10 individuals (in
609 vivo) and 3 (-)-epicatechin metabolites or its equimolar mix (in vitro). The heatmap represents the
610 -log10(p-value) of the enriched pathways. Pathways were ranked by the sum of -log10(p-values).
611
612
613 **Figure 7: Comparison (-)-epicatechin diet intervention DMPs with atherosclerosis related**
614 **athDMP.** A) Comparison of delta beta values atherosclerosis/healthy (athero-DMPs, X-axis) and
615 delta beta values after (-)-epicatechin diet intervention (Y-axis). Red CpG probes are those athero-
616 DMPs which were reversed by the (-)-epicatechin diet intervention. **B)** Correlation of the delta beta
617 values between atherosclerosis and (-)-epicatechin diet for every individual. **C)** Comparison of the
618 correlation coefficient between atherosclerosis and diet effect (X-axis) and estimated granulocyte
619 (left) and CD4+ T-cell fraction (Y-axis).

Figure 8: Pearson correlation of individual epigenetic response to (-)-epicatechin diet intervention versus corresponding vascular health biomarker measurements. A) Pearson correlation of individual (-)-epicatechin diet DMPs vs athDMPs against corresponding vascular health biomarker measurements. B) Pearson correlation of individual number of (-)-epicatechin diet DMPs against corresponding vascular health biomarker measurements. Vascular health markers were grouped in different categories (blood.cell.counts, GE.inflammatory, etc).

Table legends

Table 1: **mm-GBSA binding energy (ΔG, kcal/mol) of molecules to (A) DNMT1 and (B) DNMT3A**

Table 2: Reciprocal TNF and (-)-epicatechin gene associated DMPs cluster 1

Table 3: Reciprocal TNF and (-)-epicatechin gene associaterd DMPs cluster 2

Conflict of interest

The authors have no conflict of interest

Financial support

This work was funded by the European Union project "Flaviola", grant number 226588, within the Seventh Framework Program (http://www.flaviola.org) and COST Action NutRedOx-CA16112 supported by COST (European Cooperation in Science and Technology).

Acknowledgement

We thank the Mars Inc. for providing us with metabolites.

659 **References**

660

661 [1] D. Del Rio, A. Rodriguez-Mateos, J.P. Spencer, M. Tognolini, G. Borges, A. Crozier, Dietary
662 (poly)phenolics in human health: structures, bioavailability, and evidence of protective effects
663 against chronic diseases, Antioxidants & redox signaling 18(14) (2013) 1818-92.
664 [2] J.I. Dower, J.M. Geleijnse, P. Hollman, S.S. Soedamah-Muthu, D. Kromhout, Dietary
665 epicatechin intake and 25-y risk of cardiovascular mortality: the Zutphen Elderly Study, The
666 American journal of clinical nutrition 104(1) (2016) 58-64.
667 [3] A. Vogiatzoglou, A.A. Mulligan, A. Bhaniani, M.A.H. Lentjes, A. McTaggart, R.N. Luben, C.
668 Heiss, M. Kelm, M.W. Merx, J.P.E. Spencer, H. Schroeter, K.T. Khaw, G.G.C. Kuhnle,
669 Associations between flavan-3-ol intake and CVD risk in the Norfolk cohort of the European
670 Prospective Investigation into Cancer (EPIC-Norfolk), Free Radic Biol Med 84 (2015) 1-10.
671 [4] J.I. Ottaviani, G. Borges, T.Y. Momma, J.P. Spencer, C.L. Keen, A. Crozier, H. Schroeter, The
672 metabolome of [2-(14)C](-)-epicatechin in humans: implications for the assessment of efficacy,
673 safety, and mechanisms of action of polyphenolic bioactives, Scientific reports 6 (2016) 29034.
674 [5] J.I. Ottaviani, C. Heiss, J.P.E. Spencer, M. Kelm, H. Schroeter, Recommending flavanols and
675 procyanidins for cardiovascular health: Revisited, Mol Aspects Med 61 (2018) 63-75.
676 [6] T. De Bruyne, B. Steenput, L. Roth, G.R.Y. De Meyer, C.N.D. Santos, K. Valentova, M.
677 Dambrova, N. Hermans, Dietary Polyphenols Targeting Arterial Stiffness: Interplay of
678 Contributing Mechanisms and Gut Microbiome-Related Metabolism, Nutrients 11(3) (2019).
679 [7] H. Schroeter, C. Heiss, J. Balzer, P. Kleinbongard, C.L. Keen, N.K. Hollenberg, H. Sies, C.
680 Kwik-Uribe, H.H. Schmitz, M. Kelm, (-)-Epicatechin mediates beneficial effects of flavanol-rich
681 cocoa on vascular function in humans, Proceedings of the National Academy of Sciences of the
682 United States of America 103(4) (2006) 1024-9.
683 [8] S. Desch, J. Schmidt, D. Kobler, M. Sonnabend, I. Eitel, M. Sareban, K. Rahimi, G. Schuler,
684 H. Thiele, Effect of cocoa products on blood pressure: systematic review and meta-analysis,
685 American journal of hypertension 23(1) (2010) 97-103.
686 [9] A. Rodriguez-Mateos, T. Weber, S.S. Skene, J.I. Ottaviani, A. Crozier, M. Kelm, H. Schroeter,
687 C. Heiss, Assessing the respective contributions of dietary flavanol monomers and procyanidins in
688 mediating cardiovascular effects in humans: randomized, controlled, double-masked intervention
689 trial, Am J Clin Nutr 108(6) (2018) 1229-1237.
690 [10] T. Rassaf, C. Rammos, U.B. Hendgen-Cotta, C. Heiss, W. Kleophas, F. Dellanna, J. Floege,
691 G.R. Hetzel, M. Kelm, Vasculoprotective Effects of Dietary Cocoa Flavanols in Patients on
692 Hemodialysis: A Double-Blind, Randomized, Placebo-Controlled Trial, Clinical journal of the
693 American Society of Nephrology : CJASN 11(1) (2016) 108-18.
694 [11] O.A. Tokede, J.M. Gaziano, L. Djousse, Effects of cocoa products/dark chocolate on serum
695 lipids: a meta-analysis, European journal of clinical nutrition 65(8) (2011) 879-86.
696 [12] R. Jimenez, J. Duarte, F. Perez-Vizcaino, Epicatechin: endothelial function and blood
697 pressure, Journal of agricultural and food chemistry 60(36) (2012) 8823-30.
698 [13] R. Sansone, A. Rodriguez-Mateos, J. Heuel, D. Falk, D. Schuler, R. Wagstaff, G.G. Kuhnle,
699 J.P. Spencer, H. Schroeter, M.W. Merx, M. Kelm, C. Heiss, E.U.t.F.P. Flaviola Consortium, Cocoa
700 flavanol intake improves endothelial function and Framingham Risk Score in healthy men and
701 women: a randomised, controlled, double-masked trial: the Flaviola Health Study, The British
702 journal of nutrition 114(8) (2015) 1246-55.
703 [14] I. Ramirez-Sanchez, C. Mansour, V. Navarrete-Yanez, M. Ayala-Hernandez, G. Guevara, C.
704 Castillo, M. Loredo, M. Bustamante, G. Ceballos, F.J. Villarreal, (-)-Epicatechin induced reversal

of endothelial cell aging and improved vascular function: underlying mechanisms, Food & function 9(9) (2018) 4802-4813.
[15] P. Libby, Inflammation in atherosclerosis, Nature 420(6917) (2002) 868-74.
[16] S. Claude, C. Boby, A. Rodriguez-Mateos, J.P. Spencer, N. Gerard, C. Morand, D. Milenkovic, Flavanol metabolites reduce monocyte adhesion to endothelial cells through modulation of expression of genes via p38-MAPK and p65-Nf-kB pathways, Molecular nutrition & food research 58(5) (2014) 1016-27.
[17] D. Milenkovic, W.V. Berghe, C. Morand, S. Claude, A. van de Sandt, S. Gorressen, L.E. Monfoulet, C.S. Chirumamilla, K. Declerck, K.S.V. Szic, M. Lahtela-Kakkonen, C. Gerhauser, M.W. Merx, M. Kelm, A systems biology network analysis of nutri(epi)genomic changes in endothelial cells exposed to epicatechin metabolites, Scientific reports 8(1) (2018) 15487.
[18] R. Castro, I. Rivera, C. Martins, E.A. Struys, E.E. Jansen, N. Clode, L.M. Graca, H.J. Blom, C. Jakobs, I.T. de Almeida, Intracellular S-adenosylhomocysteine increased levels are associated with DNA hypomethylation in HUVEC, Journal of molecular medicine 83(10) (2005) 831-6.
[19] Y.Z. Jiang, E. Manduchi, C.J. Stoeckert, Jr., P.F. Davies, Arterial endothelial methylome: differential DNA methylation in athero-susceptible disturbed flow regions in vivo, BMC genomics 16 (2015) 506.
[20] X. Yu, W. Ling, M. Mi, Relationship of impairment induced by intracellular S-adenosylhomocysteine accumulation with DNA methylation in human umbilical vein endothelial cells treated with 3-deazaadenosine, International journal of experimental pathology 90(6) (2009) 638-48.
[21] V.C. George, G. Dellaire, H.P.V. Rupasinghe, Plant flavonoids in cancer chemoprevention: role in genome stability, The Journal of nutritional biochemistry 45 (2017) 1-14.
[22] K. Szarc Vel Szic, K. Declerck, R.A.J. Crans, J. Diddens, D.B. Scherf, C. Gerhauser, W. Vanden Berghe, Epigenetic silencing of triple negative breast cancer hallmarks by Withaferin A, Oncotarget 8(25) (2017) 40434-40453.
[23] G. Istas, K. Declerck, M. Pudenz, K.S.V. Szic, V. Lendinez-Tortajada, M. Leon-Latre, K. Heyninck, G. Haegeman, J.A. Casasnovas, M. Tellez-Plaza, C. Gerhauser, C. Heiss, A. Rodriguez-Mateos, W.V. Berghe, Identification of differentially methylated BRCA1 and CRISP2 DNA regions as blood surrogate markers for cardiovascular disease, Sci Rep 7(1) (2017) 5120.
[24] D. Milenkovic, W. Vanden Berghe, C. Boby, C. Leroux, K. Declerck, K. Szarc vel Szic, K. Heyninck, K. Laukens, M. Bizet, M. Defrance, S. Dedeurwaerder, E. Calonne, F. Fuks, G. Haegeman, G.R. Haenen, A. Bast, A.R. Weseler, Dietary flavanols modulate the transcription of genes associated with cardiovascular pathology without changes in their DNA methylation state, PLoS One 9(4) (2014) e95527.
[25] Y. Assenov, F. Muller, P. Lutsik, J. Walter, T. Lengauer, C. Bock, Comprehensive analysis of DNA methylation data with RnBeads, Nature methods 11(11) (2014) 1138-1140.
[26] A.E. Teschendorff, F. Marabita, M. Lechner, T. Bartlett, J. Tegner, D. Gomez-Cabrero, S. Beck, A beta-mixture quantile normalization method for correcting probe design bias in Illumina Infinium 450 k DNA methylation data, Bioinformatics 29(2) (2013) 189-96.
[27] E.A. Houseman, W.P. Accomando, D.C. Koestler, B.C. Christensen, C.J. Marsit, H.H. Nelson, J.K. Wiencke, K.T. Kelsey, DNA methylation arrays as surrogate measures of cell mixture distribution, BMC Bioinformatics 13 (2012) 86.
[28] A.E. Teschendorff, C.E. Breeze, S.C. Zheng, S. Beck, A comparison of reference-based algorithms for correcting cell-type heterogeneity in Epigenome-Wide Association Studies, BMC Bioinformatics 18(1) (2017) 105.

[29] S. Horvath, DNA methylation age of human tissues and cell types, Genome Biol 14(10) (2013) R115.
[30] D. Stöckel, T. Kehl, P. Trampert, L. Schneider, C. Backes, N. Ludwig, A. Gerasch, M. Kaufmann, M. Gessler, N. Graf, E. Meese, A. Keller, H.-P. Lenhof, Multi-omics enrichment analysis using the GeneTrail2 web service, Bioinformatics 32(10) (2016) 1502-1508.
[31] Y. Zhou, B. Zhou, L. Pache, M. Chang, A.H. Khodabakhshi, O. Tanaseichuk, C. Benner, S.K. Chanda, Metascape provides a biologist-oriented resource for the analysis of systems-level datasets, Nature Communications 10(1) (2019) 1523.
[32] P. Shannon, A. Markiel, O. Ozier, N.S. Baliga, J.T. Wang, D. Ramage, N. Amin, B. Schwikowski, T. Ideker, Cytoscape: a software environment for integrated models of biomolecular interaction networks, Genome research 13(11) (2003) 2498-504.
[33] M.Z. Fang, Y. Wang, N. Ai, Z. Hou, Y. Sun, H. Lu, W. Welsh, C.S. Yang, Tea polyphenol (-)-epigallocatechin-3-gallate inhibits DNA methyltransferase and reactivates methylation-silenced genes in cancer cell lines, Cancer research 63(22) (2003) 7563-70.
[34] W.J. Lee, J.Y. Shim, B.T. Zhu, Mechanisms for the inhibition of DNA methyltransferases by tea catechins and bioflavonoids, Mol Pharmacol 68(4) (2005) 1018-30.
[35] T. Hou, J. Wang, Y. Li, W. Wang, Assessing the performance of the molecular mechanics/Poisson Boltzmann surface area and molecular mechanics/generalized Born surface area methods. II. The accuracy of ranking poses generated from docking, Journal of computational chemistry 32(5) (2011) 866-77.
[36] L. Actis-Goretta, A. Leveques, F. Giuffrida, F. Romanov-Michailidis, F. Viton, D. Barron, M. Duenas-Paton, S. Gonzalez-Manzano, C. Santos-Buelga, G. Williamson, F. Dionisi, Elucidation of (-)-epicatechin metabolites after ingestion of chocolate by healthy humans, Free Radic Biol Med 53(4) (2012) 787-95.
[37] C.G. Fraga, P.I. Oteiza, Dietary flavonoids: Role of (-)-epicatechin and related procyanidins in cell signaling, Free Radic Biol Med 51(4) (2011) 813-23.
[38] J.I. Ottaviani, T.Y. Momma, C. Heiss, C. Kwik-Uribe, H. Schroeter, C.L. Keen, The stereochemical configuration of flavanols influences the level and metabolism of flavanols in humans and their biological activity in vivo, Free Radic Biol Med 50(2) (2011) 237-44.
[39] D.M. Poitz, G. Ende, B. Stutz, A. Augstein, J. Friedrichs, C. Brunssen, C. Werner, R.H. Strasser, S. Jellinghaus, EphrinB2/EphA4-mediated activation of endothelial cells increases monocyte adhesion, Mol Immunol 68(2 Pt C) (2015) 648-56.
[40] Z. Lin, J. Jin, W. Bai, J. Li, X. Shan, Netrin-1 prevents the attachment of monocytes to endothelial cells via an anti-inflammatory effect, Mol Immunol 103 (2018) 166-172.
[41] T. Okamoto, K. Suzuki, The Role of Gap Junction-Mediated Endothelial Cell-Cell Interaction in the Crosstalk between Inflammation and Blood Coagulation, Int J Mol Sci 18(11) (2017).
[42] S. Hu, Y. Liu, T. You, J. Heath, L. Xu, X. Zheng, A. Wang, Y. Wang, F. Li, F. Yang, Y. Cao, H. Zhang, J.M. van Gils, A.J. van Zonneveld, H. Jo, Q. Wu, Y. Zhang, C. Tang, L. Zhu, Vascular Semaphorin 7A Upregulation by Disturbed Flow Promotes Atherosclerosis Through Endothelial beta1 Integrin, Arterioscler Thromb Vasc Biol 38(2) (2018) 335-343.
[43] S. Hu, L. Zhu, Semaphorins and Their Receptors: From Axonal Guidance to Atherosclerosis, Front Physiol 9 (2018) 1236.
[44] X.P. Wang, Z.Y. Cheng, K.L. Schmid, GABAB receptors expressed in human aortic endothelial cells mediate intracellular calcium concentration regulation and endothelial nitric oxide synthase translocation, Biomed Res Int 2014 (2014) 871735.

[45] Z. Zhu, Z. Shi, C. Xie, W. Gong, Z. Hu, Y. Peng, A novel mechanism of Gamma-aminobutyric acid (GABA) protecting human umbilical vein endothelial cells (HUVECs) against H2O2-induced oxidative injury, Comp Biochem Physiol C Toxicol Pharmacol 217 (2019) 68-75.
[46] M.C. Litterio, G. Jaggers, G. Sagdicoglu Celep, A.M. Adamo, M.A. Costa, P.I. Oteiza, C.G. Fraga, M. Galleano, Blood pressure-lowering effect of dietary (-)-epicatechin administration in L-NAME-treated rats is associated with restored nitric oxide levels, Free Radic Biol Med 53(10) (2012) 1894-902.
[47] A.J. Flammer, I. Sudano, M. Wolfrum, R. Thomas, F. Enseleit, D. Periat, P. Kaiser, A. Hirt, M. Hermann, M. Serafini, A. Leveques, T.F. Luscher, F. Ruschitzka, G. Noll, R. Corti, Cardiovascular effects of flavanol-rich chocolate in patients with heart failure, Eur Heart J 33(17) (2012) 2172-80.
[48] A. Nehme, K. Zibara, Cellular distribution and interaction between extended renin-angiotensin-aldosterone system pathways in atheroma, Atherosclerosis 263 (2017) 334-342.
[49] A. Knutsson, S. Hsiung, S. Celik, S. Rattik, I.Y. Mattisson, M. Wigren, H.I. Scher, J. Nilsson, A. Hultgardh-Nilsson, Treatment with a GnRH receptor agonist, but not the GnRH receptor antagonist degarelix, induces atherosclerotic plaque instability in ApoE(-/-) mice, Sci Rep 6 (2016) 26220.
[50] T. Qiu, D. Wu, L. Yang, H. Ye, Q. Wang, Z. Cao, K. Tang, Exploring the Mechanism of Flavonoids Through Systematic Bioinformatics Analysis, Front Pharmacol 9 (2018) 918.
[51] I.A. Siddiqui, M. Asim, B.B. Hafeez, V.M. Adhami, R.S. Tarapore, H. Mukhtar, Green tea polyphenol EGCG blunts androgen receptor function in prostate cancer, FASEB J 25(4) (2011) 1198-207.
[52] L.Z. Zhang, S. Lei, Changes of junctions of endothelial cells in coronary sclerosis: A review, Chronic Dis Transl Med 2(1) (2016) 22-26.
[53] D.A. Chistiakov, A.N. Orekhov, Y.V. Bobryshev, Endothelial Barrier and Its Abnormalities in Cardiovascular Disease, Front Physiol 6 (2015) 365.
[54] L.Y. Fong, C.T. Ng, Y.K. Yong, M.N. Hakim, Z. Ahmad, Asiatic acid stabilizes cytoskeletal proteins and prevents TNF-alpha-induced disorganization of cell-cell junctions in human aortic endothelial cells, Vascul Pharmacol 117 (2019) 15-26.
[55] M. Amasheh, A. Fromm, S.M. Krug, S. Amasheh, S. Andres, M. Zeitz, M. Fromm, J.D. Schulzke, TNFalpha-induced and berberine-antagonized tight junction barrier impairment via tyrosine kinase, Akt and NFkappaB signaling, J Cell Sci 123(Pt 23) (2010) 4145-55.
[56] A.A. Bhat, S. Uppada, I.W. Achkar, S. Hashem, S.K. Yadav, M. Shanmugakonar, H.A. Al-Naemi, M. Haris, S. Uddin, Tight Junction Proteins and Signaling Pathways in Cancer and Inflammation: A Functional Crosstalk, Front Physiol 9 (2018) 1942.
[57] I. Werner, F. Guo, A.H. Kiessling, E. Juengel, B. Relja, P. Lamm, U.A. Stock, A. Moritz, A. Beiras-Fernandez, Treatment of endothelial cell with flavonoids modulates transendothelial leukocyte migration, Phlebology 30(6) (2015) 405-11.
[58] A.R. Weseler, E.J. Ruijters, M.J. Drittij-Reijnders, K.D. Reesink, G.R. Haenen, A. Bast, Pleiotropic benefit of monomeric and oligomeric flavanols on vascular health--a randomized controlled clinical pilot study, PLoS One 6(12) (2011) e28460.
[59] L.E. Reinius, N. Acevedo, M. Joerink, G. Pershagen, S.E. Dahlen, D. Greco, C. Soderhall, A. Scheynius, J. Kere, Differential DNA methylation in purified human blood cells: implications for cell lineage and studies on disease susceptibility, PLoS One 7(7) (2012) e41361.
[60] M. Gomez-Guzman, R. Jimenez, M. Sanchez, M.J. Zarzuelo, P. Galindo, A.M. Quintela, R. Lopez-Sepulveda, M. Romero, J. Tamargo, F. Vargas, F. Perez-Vizcaino, J. Duarte, Epicatechin lowers blood pressure, restores endothelial function, and decreases oxidative stress and endothelin-

1 and NADPH oxidase activity in DOCA-salt hypertension, Free Radic Biol Med 52(1) (2012) 70-9.
[61] N. Ardanaz, X.P. Yang, M.E. Cifuentes, M.J. Haurani, K.W. Jackson, T.D. Liao, O.A. Carretero, P.J. Pagano, Lack of glutathione peroxidase 1 accelerates cardiac-specific hypertrophy and dysfunction in angiotensin II hypertension, Hypertension 55(1) (2010) 116-23.
[62] V. Saio, D. Syiem, R. Sharma, J. Dkhar, Amelioration of age-dependent increase in oxidative stress markers in male mice by extract of Potentilla fulgens, Redox Rep 21(3) (2016) 130-8.
[63] T. Yang, X. Li, W. Zhu, C. Chen, Z. Sun, Z. Tan, J. Kang, Alteration of antioxidant enzymes and associated genes induced by grape seed extracts in the primary muscle cells of goats in vitro, PLoS One 9(9) (2014) e107670.
[64] B. Delatte, J. Jeschke, M. Defrance, M. Bachman, C. Creppe, E. Calonne, M. Bizet, R. Deplus, L. Marroqui, M. Libin, M. Ravichandran, F. Mascart, D.L. Eizirik, A. Murrell, T.P. Jurkowski, F. Fuks, Genome-wide hydroxymethylcytosine pattern changes in response to oxidative stress, Sci Rep 5 (2015) 12714.
[65] K. Declerck, K. Szarc vel Szic, A. Palagani, K. Heyninck, G. Haegeman, C. Morand, D. Milenkovic, W. Vanden Berghe, Epigenetic control of cardiovascular health by nutritional polyphenols involves multiple chromatin-modifying writer-reader-eraser proteins, Curr Top Med Chem 16(7) (2016) 788-806.
[66] H.K. Komori, T. Hart, S.A. LaMere, P.V. Chew, D.R. Salomon, Defining CD4 T cell memory by the epigenetic landscape of CpG DNA methylation, J Immunol 194(4) (2015) 1565-79.
[67] P. Ji, X. Wang, N. Xie, Y. Li, N6-Methyladenosine in RNA and DNA: An Epitranscriptomic and Epigenetic Player Implicated in Determination of Stem Cell Fate, Stem Cells Int 2018 (2018) 3256524.
[68] A.K. Maunakea, I. Chepelev, K. Cui, K. Zhao, Intragenic DNA methylation modulates alternative splicing by recruiting MeCP2 to promote exon recognition, Cell Res 23(11) (2013) 1256-69.
[69] S.M. Linker, L. Urban, S.J. Clark, M. Chhatriwala, S. Amatya, D.J. McCarthy, I. Ebersberger, L. Vallier, W. Reik, O. Stegle, M.J. Bonder, Combined single-cell profiling of expression and DNA methylation reveals splicing regulation and heterogeneity, Genome Biol 20(1) (2019) 30.
[70] S. Singh, S.P. Narayanan, K. Biswas, A. Gupta, N. Ahuja, S. Yadav, R.K. Panday, A. Samaiya, S.K. Sharan, S. Shukla, Intragenic DNA methylation and BORIS-mediated cancer-specific splicing contribute to the Warburg effect, Proc Natl Acad Sci U S A 114(43) (2017) 11440-11445.
[71] T.V. Ramanouskaya, V.V. Grinev, The determinants of alternative RNA splicing in human cells, Mol Genet Genomics 292(6) (2017) 1175-1195.
[72] R. Aversa, A. Sorrentino, R. Esposito, M.R. Ambrosio, A. Amato, A. Zambelli, A. Ciccodicola, L. D'Apice, V. Costa, Alternative Splicing in Adhesion- and Motility-Related Genes in Breast Cancer, Int J Mol Sci 17(1) (2016).
[73] L. Zhong, M.J. Simard, J. Huot, Endothelial microRNAs regulating the NF-kappaB pathway and cell adhesion molecules during inflammation, FASEB J 32(8) (2018) 4070-4084.
[74] X. Tzounis, A. Rodriguez-Mateos, J. Vulevic, G.R. Gibson, C. Kwik-Uribe, J.P. Spencer, Prebiotic evaluation of cocoa-derived flavanols in healthy humans by using a randomized, controlled, double-blind, crossover intervention study, Am J Clin Nutr 93(1) (2011) 62-72.
[75] A. Rodriguez-Mateos, T. Cifuentes-Gomez, I. Gonzalez-Salvador, J.I. Ottaviani, H. Schroeter, M. Kelm, C. Heiss, J.P. Spencer, Influence of age on the absorption, metabolism, and excretion of cocoa flavanols in healthy subjects, Mol Nutr Food Res 59(8) (2015) 1504-12.

[76] T. Angkananard, T. Anothaisintawee, A. Ingsathit, M. McEvoy, K. Silapat, J. Attia, P. Sritara, A. Thakkinstian, Mediation Effect of Neutrophil Lymphocyte Ratio on Cardiometabolic Risk Factors and Cardiovascular Events, Sci Rep 9(1) (2019) 2618.
[77] Y.H. Jhuang, T.W. Kao, T.C. Peng, W.L. Chen, Y.W. Li, P.K. Chang, L.W. Wu, Neutrophil to lymphocyte ratio as predictor for incident hypertension: a 9-year cohort study in Taiwan, Hypertens Res 42(8) (2019) 1209-1214.
[78] E. Huguet, G. Maccallini, P. Pardini, M. Hidalgo, S. Obregon, F. Botto, M. Koretzky, P.M. Nilsson, K. Ferdinand, C. Kotliar, Reference Values for Neutrophil to Lymphocyte Ratio (NLR), a Biomarker of Cardiovascular Risk, According to Age and Sex in a Latin American Population, Curr Probl Cardiol (2019).
[79] A.C. Aykan, E. Hatem, E. Kalaycioglu, C.Y. Karabay, R. Zehir, T. Gokdeniz, D. Altintas Aykan, S. Celik, Neutrophil-to-lymphocyte ratio may be a marker of peripheral artery disease complexity, Anatol J Cardiol 16(7) (2016) 497-503.
[80] D.C. Koestler, J. Usset, B.C. Christensen, C.J. Marsit, M.R. Karagas, K.T. Kelsey, J.K. Wiencke, DNA Methylation-Derived Neutrophil-to-Lymphocyte Ratio: An Epigenetic Tool to Explore Cancer Inflammation and Outcomes, Cancer Epidemiol Biomarkers Prev 26(3) (2017) 328-338.
[81] S. Ligthart, C. Marzi, S. Aslibekyan, M.M. Mendelson, K.N. Conneely, T. Tanaka, E. Colicino, L.L. Waite, R. Joehanes, W. Guan, J.A. Brody, C. Elks, R. Marioni, M.A. Jhun, G. Agha, J. Bressler, C.K. Ward-Caviness, B.H. Chen, T. Huan, K. Bakulski, E.L. Salfati, W.-E. Investigators, G. Fiorito, C.e.o.C.H. Disease, S. Wahl, K. Schramm, J. Sha, D.G. Hernandez, A.C. Just, J.A. Smith, N. Sotoodehnia, L.C. Pilling, J.S. Pankow, P.S. Tsao, C. Liu, W. Zhao, S. Guarrera, V.J. Michopoulos, A.K. Smith, M.J. Peters, D. Melzer, P. Vokonas, M. Fornage, H. Prokisch, J.C. Bis, A.Y. Chu, C. Herder, H. Grallert, C. Yao, S. Shah, A.F. McRae, H. Lin, S. Horvath, D. Fallin, A. Hofman, N.J. Wareham, K.L. Wiggins, A.P. Feinberg, J.M. Starr, P.M. Visscher, J.M. Murabito, S.L. Kardia, D.M. Absher, E.B. Binder, A.B. Singleton, S. Bandinelli, A. Peters, M. Waldenberger, G. Matullo, J.D. Schwartz, E.W. Demerath, A.G. Uitterlinden, J.B. van Meurs, O.H. Franco, Y.I. Chen, D. Levy, S.T. Turner, I.J. Deary, K.J. Ressler, J. Dupuis, L. Ferrucci, K.K. Ong, T.L. Assimes, E. Boerwinkle, W. Koenig, D.K. Arnett, A.A. Baccarelli, E.J. Benjamin, A. Dehghan, DNA methylation signatures of chronic low-grade inflammation are associated with complex diseases, Genome Biol 17(1) (2016) 255.
[82] R. Wang, P.J. Chen, W.H. Chen, Diet and exercise improve neutrophil to lymphocyte ratio in overweight adolescents, Int J Sports Med 32(12) (2011) 982-6.
[83] F. Palmacci, E. Toti, A. Raguzzini, G. Catasta, P. Aiello, I. Peluso, M. Biava, M. Palmery, Neutrophil-to-Lymphocyte Ratio, Mediterranean Diet, and Bone Health in Coeliac Disease Patients: A Pilot Study, Oxid Med Cell Longev 2019 (2019) 7384193.
[84] A. Syauqy, C.Y. Hsu, H.H. Rau, J.C. Chao, Association of dietary patterns, anthropometric measurements, and metabolic parameters with C-reactive protein and neutrophil-to-lymphocyte ratio in middle-aged and older adults with metabolic syndrome in Taiwan: a cross-sectional study, Nutr J 17(1) (2018) 106.
[85] A. Sut, M. Pytel, M. Zadrozny, J. Golanski, M. Rozalski, Polyphenol-rich diet is associated with decreased level of inflammatory biomarkers in breast cancer patients, Rocz Panstw Zakl Hig 70(2) (2019) 177-184.
[86] G. Pounis, M. Bonaccio, A. Di Castelnuovo, S. Costanzo, A. de Curtis, M. Persichillo, S. Sieri, M.B. Donati, C. Cerletti, G. de Gaetano, L. Iacoviello, Polyphenol intake is associated with low-grade inflammation, using a novel data analysis from the Moli-sani study, Thromb Haemost 115(2) (2016) 344-52.

[87] O.K. Chun, S.J. Chung, K.J. Claycombe, W.O. Song, Serum C-reactive protein concentrations are inversely associated with dietary flavonoid intake in U.S. adults, J Nutr 138(4) (2008) 753-60.
[88] R. di Giuseppe, A. Di Castelnuovo, F. Centritto, F. Zito, A. De Curtis, S. Costanzo, B. Vohnout, S. Sieri, V. Krogh, M.B. Donati, G. de Gaetano, L. Iacoviello, Regular consumption of dark chocolate is associated with low serum concentrations of C-reactive protein in a healthy Italian population, J Nutr 138(10) (2008) 1939-45.
[89] R. Schnabel, K.J. Lackner, H.J. Rupprecht, C. Espinola-Klein, M. Torzewski, E. Lubos, C. Bickel, F. Cambien, L. Tiret, T. Munzel, S. Blankenberg, Glutathione peroxidase-1 and homocysteine for cardiovascular risk prediction: results from the AtheroGene study, J Am Coll Cardiol 45(10) (2005) 1631-7.
[90] R. Esse, M. Barroso, I. Tavares de Almeida, R. Castro, The Contribution of Homocysteine Metabolism Disruption to Endothelial Dysfunction: State-of-the-Art, Int J Mol Sci 20(4) (2019).
[91] A. Gottsater, I. Anwaar, K.F. Eriksson, I. Mattiasson, F. Lindgarde, Homocysteine is related to neopterin and endothelin-1 in plasma of subjects with disturbed glucose metabolism and reference subjects, Angiology 51(6) (2000) 489-97.
[92] J. Hamelet, K. Demuth, J. Dairou, A. Ledru, J.L. Paul, J.M. Dupret, J.M. Delabar, F. Rodrigues-Lima, N. Janel, Effects of catechin on homocysteine metabolism in hyperhomocysteinemic mice, Biochem Biophys Res Commun 355(1) (2007) 221-7.
[93] X. Gao, M. Jia, Y. Zhang, L.P. Breitling, H. Brenner, DNA methylation changes of whole blood cells in response to active smoking exposure in adults: a systematic review of DNA methylation studies, Clin Epigenetics 7 (2015) 113.
[94] O. Hahn, L. Drews, A. Nguyen, T. Tatsuta, L. Gkioni, O. Hendrich, Q. Zhang, T. Langer, S. Pletcher, M. Wakelam, A. Beyer, S. Grönke, L. Partridge, A nutritional memory effect counteracts the benefits of dietary restriction in old mice, Nature metabolism doi:10.1038/s42255-019-0121-0 (2019).

962 **Table 1**: mm-GBSA binding energy (ΔG, kcal/mol) of molecules to (A) DNMT1 and (B)
963 DNMT3A

(A)	DNA binding site	Catalytic domain (I)	Catalytic domain (II)
(-)-epicatechin	-31.82	-32.07	-37.95
3'MEC	-32.82	-23.79	-36.18
EC4'S	-35.14	-24.56	-34.79
4MEC7G	-46.24	-38.72	-55.43
Sucrose	-24.47	-36.82	-36.97
Naphthalene	-13.62	-8.3	-20.67

964

(B)	PWWP domain	H3 peptide binding site	DNMT3A binding site	DNMT3L binding site
(-)-epicatechin	-48.34	-26.50	-31.24	-29.76
3'MEC	-38.23	-28.81	-29.70	-22.93
EC4'S	-42.10	-17.35	-26.70	-31.34
4MEC7G	-51.72	-36.81	-55.42	-33.10
Sucrose	-30.37	-9.20	-34.01	-20.27
Naphthalene	-30.77	-8.11	-22.52	-19.33

965

966

Table 2

Genes cluster 1	treatment	Δβ versus TNF	Δβ versus Ctrl	P.Value	cgProbe_ID	β_control	β_TNF	β_4'MEC	β_4'MEC7G	β_EC4'S
PCDH9	4'MEC	0,08		0,009	cg20212077	0,38	0,34	0,42	0,42	0,39
	4'MEC7G+TNF	0,08		0,008	cg20212077	0,38	0,34	0,42	0,42	0,39
	EC4'S	0,06		0,008	cg16184802	0,81	0,78	0,79	0,84	0,85
	TNF		-0,06	0,007	cg15566921	0,98	0,92	0,97	0,93	0,95
DLGAP2	4'MEC	0,08		0,003	cg06452558	0,49	0,47	0,56	0,53	0,53
	4'MEC7G+TNF	0,06		0,004	cg15961904	0,86	0,86	0,88	0,92	0,88
	4'MEC7G+TNF	0,06		0,009	cg05455971	0,71	0,72	0,72	0,78	0,75
	EC4'S	0,07		0,006	cg00579531	0,68	0,65	0,66	0,69	0,72
	EC4'S	0,06		0,008	cg02095946	0,90	0,89	0,92	0,92	0,94
	TNF		-0,05	0,006	cg03308704	0,95	0,90	0,92	0,94	0,93
SDK1	4'MEC	0,06		0,009	cg25783987	0,84	0,83	0,90	0,85	0,83
	4'MEC7G+TNF	0,06		0,009	cg04534231	0,81	0,81	0,82	0,88	0,87
	EC4'S	0,07		0,006	cg19569074	0,65	0,63	0,66	0,64	0,70
	TNF		-0,06	0,001	cg11998431	0,92	0,86	0,87	0,88	0,89
BANP	4'MEC	0,06		0,002	cg06173520	0,93	0,87	0,93	0,93	0,91
	4'MEC7G+TNF	0,06		0,007	cg06173520	0,93	0,87	0,93	0,93	0,91
	EC4'S	0,07		0,002	cg00935421	0,80	0,82	0,84	0,85	0,89
	TNF		-0,06	0,003	cg06173520	0,93	0,87	0,93	0,93	0,91
KDM2B	4'MEC	0,06		0,009	cg16062733	0,75	0,69	0,75	0,77	0,78
	4'MEC7G+TNF	0,08		0,001	cg16062733	0,75	0,69	0,75	0,77	0,78
	EC4'S	0,09		0,001	cg16062733	0,75	0,69	0,75	0,77	0,78
	TNF		-0,05	0,010	cg16062733	0,75	0,69	0,75	0,77	0,78

Table 3

Genes cluster 2	treatment	Δβ versus TNF	Δβ versus Ctrl	P.Value	cgProbe_ID	β_control	β_TNF	β_4'MEC	β_4'MEC7G	β_EC4'S
AKAP12	4'MEC	-0,06		0,003	cg21047322	0,86	0,92	0,86	0,85	0,86
	4'MEC7G+TNF	-0,07		0,001	cg21047322	0,86	0,92	0,86	0,85	0,86
	EC4'S	-0,06		0,006	cg21047322	0,86	0,92	0,86	0,85	0,86
	TNF		0,06	0,002	cg21047322	0,86	0,92	0,86	0,85	0,86
LAS1L	4'MEC	-0,06		0,002	cg17299883	0,13	0,18	0,12	0,12	0,12
	4'MEC7G+TNF	-0,07		0,001	cg17299883	0,13	0,18	0,12	0,12	0,12
	EC4'S	-0,06		0,002	cg17299883	0,13	0,18	0,12	0,12	0,12
	TNF		0,05	0,004	cg17299883	0,13	0,18	0,12	0,12	0,12
USP35	4'MEC	-0,07		0,002	cg15243034	0,78	0,86	0,80	0,79	0,80
	4'MEC7G+TNF	-0,08		0,001	cg15243034	0,78	0,86	0,80	0,79	0,80
	EC4'S	-0,06		0,003	cg15243034	0,78	0,86	0,80	0,79	0,80
	TNF		0,09	0,000	cg15243034	0,78	0,86	0,80	0,79	0,80
GLUD1P3	4'MEC	-0,07		0,008	cg02005425	0,73	0,82	0,75	0,73	0,72
	4'MEC7G+TNF	-0,09		0,002	cg02005425	0,73	0,82	0,75	0,73	0,72
	EC4'S	-0,10		0,001	cg02005425	0,73	0,82	0,75	0,73	0,72
	TNF		0,09	0,001	cg02005425	0,73	0,82	0,75	0,73	0,72
PTCHD3	4'MEC	-0,09		0,003	cg10599633	0,85	0,91	0,83	0,79	0,85
	4'MEC7G+TNF	-0,12		0,000	cg10599633	0,85	0,91	0,83	0,79	0,85
	EC4'S	-0,07		0,009	cg10599633	0,85	0,91	0,83	0,79	0,85
	TNF		0,06	0,008	cg10599633	0,85	0,91	0,83	0,79	0,85
NLGN1	4'MEC	-0,08		0,006	cg06097077	0,54	0,63	0,54	0,56	0,56
	4'MEC7G+TNF	-0,06		0,004	cg04981409	0,88	0,91	0,89	0,85	0,88
	EC4'S	-0,10		0,007	cg03417233	0,83	0,83	0,79	0,81	0,74
	TNF		0,09	0,002	cg06097077	0,54	0,63	0,54	0,56	0,56
SKI	4'MEC	-0,12		0,000	cg11191979	0,89	0,95	0,83	0,89	0,86
	4'MEC7G+TNF	-0,05		0,004	cg11191979	0,89	0,95	0,83	0,89	0,86
	EC4'S	-0,09		0,000	cg11191979	0,89	0,95	0,83	0,89	0,86
	TNF		0,06	0,001	cg11191979	0,89	0,95	0,83	0,89	0,86
XKR4	4'MEC	-0,10		0,000	cg14552904	0,77	0,83	0,73	0,79	0,70
	4'MEC7G+TNF	-0,07		0,002	cg19887883	0,89	0,93	0,90	0,86	0,91
	EC4'S	-0,13		0,000	cg14552904	0,77	0,83	0,73	0,79	0,70
	TNF		0,06	0,004	cg14552904	0,77	0,83	0,73	0,79	0,70
FLJ38576	4'MEC	-0,15		0,000	cg10631544	0,86	0,94	0,80	0,81	0,85
	4'MEC7G+TNF	-0,13		0,000	cg10631544	0,86	0,94	0,80	0,81	0,85
	EC4'S	-0,09		0,002	cg10631544	0,86	0,94	0,80	0,81	0,85
	TNF		0,08	0,002	cg10631544	0,86	0,94	0,80	0,81	0,85
DACT1	4'MEC	-0,07		0,001	cg01617520	0,89	0,92	0,85	0,81	0,86
	4'MEC	-0,14		0,003	cg00677272	0,86	0,92	0,78	0,88	0,85
	4'MEC7G+TNF	-0,10		0,000	cg01617520	0,89	0,92	0,85	0,81	0,86
	EC4'S	-0,06		0,003	cg01617520	0,89	0,92	0,85	0,81	0,86
	TNF		0,07	0,005	cg00869962	0,62	0,70	0,67	0,69	0,70

980